Ultrasound in Med. & Biol. Vol. 17, No. 4, pp. 373–382, 1991
Printed in the U.S.A.

0301-5629/91 $3.00 + .00

●*Original Contribution*

IN UTERO MEASUREMENT OF ULTRASONICALLY INDUCED FETAL MOUSE TEMPERATURE INCREASES

K. I. CARNES, J. L. DREWNIAK[†] and F. DUNN
Bioacoustics Research Laboratory, University of Illinois, 1406 West Green Street, Urbana, IL 61801

(*Received* 24 *September* 1990; *in final form* 28 *December* 1990)

Abstract—The temperature increase in the murine fetus, exposed *in vivo* to 1 MHz ultrasound in the spatial-peak temporal-average intensity range 0.5 to 10 W/cm^2 for durations of 30 to 400 s, was determined with implanted thermocouples at 9, 12 and 15 days of gestation by a method that preserved the normal uterine environment. The results show that the temperature increase is related approximately linearly to the energy flux *It*, where *I* is the acoustic intensity and *t* is the exposure duration. The temperature increase was observed to be nearly the same for the 9- and 12-day fetuses but less for day-15 specimens, possibly due to the smaller size in early gestation and increased vascularization in later gestation. The results are compared with calculations based on a model of a pair of nested parallelpipeds for which the properties of the outer body remain unchanged, the dimensions and absorption coefficient of the inner body increase with gestational age and the perfusion constant varies with gestational age.

Key Words: **Temperature elevation, Mouse fetus, Ultrasound.**

INTRODUCTION

Heat generated as an ultrasonic wave propagates in biological tissue has long been a concern to the biomedical ultrasound community because of the possibility for producing reversible and irreversible effects. As a result of this concern, the thermal mechanism for tissue damage is perhaps the best characterized and best understood of all the ultrasound physical mechanisms of interaction. However, understanding the thermal behavior of such complex media as biological tissue, involving contributions from absorption, conduction, perfusion and scattering, is presently far from complete and much current activity is devoted to studying these kinds of details (National Council on Radiation Protection, American Institute of Ultrasound in Medicine, National Electrical Manufacturers Association, European Watchdog Committee). This lack of complete understanding is particularly disconcerting in regard to temperature elevation in the developing fetus during ultrasound clinical diagnostic procedures. Because safety concerns prevent measurement of the temperature increase directly in the human fetus, investigators and medical personnel using ultrasound devices must rely on animal studies and theoretical models to obtain such critical information.

It is known that hyperthermia is a teratological agent, which has been documented for a number of mammalian species (Edwards 1986; Miller and Ziskin 1989) including humans (Brix 1982; Smith et al. 1978). The manifestations of the teratologies are dependent upon the stage of development during which heating occurs and generally result in the production of brain, skeletal or muscular defects. Early gestation heating (*i.e.*, during organogenesis) has been shown to result in particularly severe consequences (Edwards 1986; Lele 1979).

Fetal temperature increase during a wide variety of ultrasound exposure conditions has been the focus of a number of studies. In several studies, the temperature increase was measured and reported but not compared with values expected to be produced as calculated from models (Edmonds et al. 1979; Lele 1975; Sikov et al. 1984; Stolzenberg et al. 1980). Recently, Abraham et al. (1989) measured fetal temperature increases in the exteriorized rat fetus and compared these measurements to those calculated from a spherical model.

Address correspondence to: Dr. Floyd Dunn, Bioacoustics Research Laboratory, University of Illinois, 1406 W. Green St., Urbana, IL 61801.
[†] Present address: Department of Electrical Engineering, University of Missouri-Rolla, Rolla, MO 65401.

The present study was undertaken with two factors in mind, which are considered of the greatest importance for accurate determination of fetal temperature elevation due to exposure to ultrasound. These are (1) the preservation of the gravid uterine environment, and (2) the ability to compare temperature elevation measurements with computations based upon an improved bioheat transfer model. *In vivo* temperature measurements were made during ultrasound exposure at three different gestational ages. As described later, the analytical model comprises a pair of nested rectangular parallelpipeds for which the inner volume increases in dimension and possesses a different acoustic absorption coefficient for the different gestational ages, while the outer volume remains unchanged except for the perfusion constant.

METHODS

Animal preparation

All animals used in this study were housed in the same quarters. They were maintained on a 14:10 hour light–dark schedule with food (Purina Rat Chow®) and water dispensed *ad lib.* Males were housed in close proximity to the females to ensure regular 4- to 5-day estrous cycles (Whittingham and Wood 1983). Female HSD:ICR (Harlan Sprague-Dawley, Indianapolis, IN) mice 70 to 100 days of age in proestrus or estrus, as determined by vaginal smears, were mated to proven males in the afternoon at a ratio of three females to one male. The following morning the males were removed, and pregnancy was determined by the presence of a vaginal plug or a sperm-positive vaginal smear. Pregnant females were kept three to a cage until the day of the temperature elevation measurements.

Thermocouple preparation

The temperature sensors were chromel-constantan thermocouples having lap soldered junctions 30–40 μm in diameter and axial dimensions of 300–400 μm. The ends of the chromel and constantan wires were stripped of their Teflon coatings and etched with acid to taper the original 75-μm diameter to approximately 15–20 μm at the tip, cleansed with alcohol, and tinned. The individual wires were then retained in a holding device designed for this purpose, the two ends overlapped approximately 300 μm, set in contact, and soldered. The procedure was carried out with the aid of a dissecting microscope. The junction area was then sprayed with a protective coating (Krylon Crystal Clear, Borden, Inc.), designed for electronic equipment, to waterproof the junction and to prevent oxidation. The response time of the thermocouple to an instantaneous temperature increase is less than 100 msec and does not significantly affect the measurement (Fry and Fry 1954a,b).

Experimental protocol

On the day of the measurement, days 9, 12 or 15 of gestation, the dam was anesthetized by inhalation of methoxyflurane (Metofane, Pittman-Moore). The abdominal area was then shaved and the animal placed in a specially designed holder. A circulator was mounted on the holder to maintain anesthesia during the entire measurement procedure. A midline incision was made through the skin over the abdomen and the skin was carefully dissected away, leaving the underlying peritoneal tissue intact. This procedure allows visualization of the fetuses without disruption of the gravid uterine environment. The thermocouple probes were inserted into three to four randomly selected fetuses with the aid of a 30-gauge hypodermic needle, which was removed after insertion of the thermocouple. The thermocouple wires were then attached with waterproofed set screws to a harness which fits over the animal holder. The preparation is shown in Fig. 1.

The animal holder was placed in the plexiglas exposure tank with the dam's abdomen facing the transducer and the muzzle extended out of the medium into the nose cone of the anesthesia circulator. The tank contained degassed mammalian Ringer's solution, maintained at 37°C, and was lined with

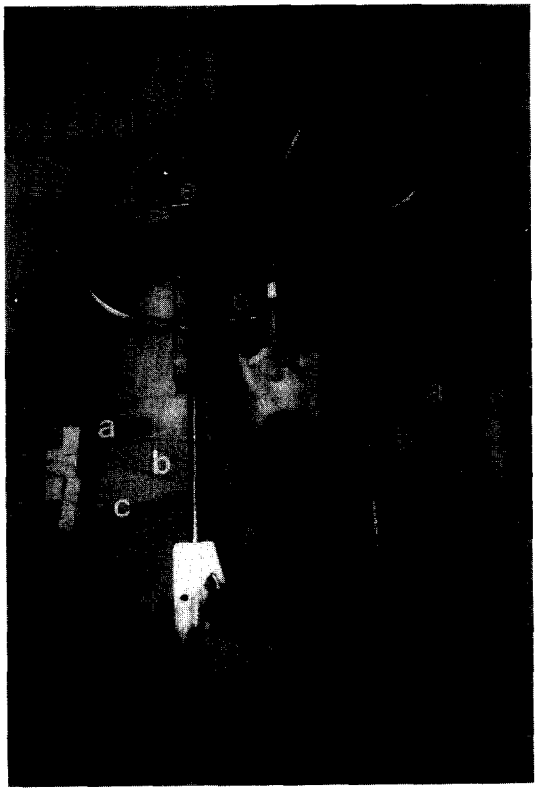

Fig. 1. Experimental animal preparation showing three thermocouple sensors (a, b and c), and the nose cone (d) for the anesthesia circulator (e).

sound-absorbing material to prevent generation of standing waves. The thermocouple wire ends were attached to bus wires leading to the amplifier.

The measurements were carried out in the far field, 25 cm from the face of the transducer. The ultrasound source was a 1-inch diameter, 1-MHz, PZT-4, unfocused ceramic transducer with a 3-dB beam width of 1.9 cm. A needle hydrophone probe (NTR Systems, Inc.) was used to determine the ultrasound beam pattern. The exposure intensities were determined in the free field in degassed mammalian Ringer's solution with a thermoelectric probe as a secondary standard that had been calibrated with a steel sphere radiometer primary standard (Dunn et al. 1977).

The harmonics in the ultrasound beam at a distance of 25 cm from the transducer, generated by nonlinear propagation, were measured with a needle hydrophone probe over the range of spatial-peak, temporal-average (SPTA) exposure intensities of 0.5 to 10 W/cm^2. The linear relation between the square of the voltage applied to the transducer and the field intensity, established by the calibration procedure at low acoustic intensities, was extrapolated for the voltages corresponding to the higher intensities. Although the SPTA intensity may deviate from the linear relation by 15% or less, at a distance of 25 cm from the transducer at high ultrasound intensities (Carstensen et al. 1980), the increased heating due to harmonic absorption can be significant (Bacon and Carstensen 1990; Carstensen et al. 1982; Dalecki et al. 1990; Fry et al. 1989; Goss and Fry 1981). The harmonics in the acoustic field, at the field position selected, were measured with a needle hydrophone probe (NTR Systems, Inc.). The second harmonic was found to be approximately 17 and 14 dB below the fundamental at 0.5 and 1 W/cm^2, respectively, and approximately 8 dB below the fundamental in the 5 to 10 W/cm^2 range. Measurements of the amplitude of the second harmonic relative to the fundamental in the 5 to 10 W/cm^2 intensity range showed only a slight increase with an increase in intensity, indicating well-developed harmonics (Blackstock 1966; Hamilton 1986; Muir and Carstensen 1980).

The absorption coefficient was measured in mouse liver over the range of SPTA intensities 1 to 10 W/cm^2 to assess the increase in the heating due to nonlinear absorption. The absorption coefficient at 10 W/cm^2 was found to be 2.3 times greater than that at 1 W/cm^2. This is consistent with other such reported measurements (Bacon and Carstensen 1990; Carstensen et al. 1989; Dalecki et al. 1990). Because the volumetric rate of energy deposition in the soft tissue is proportional to the product αI, the intensities were scaled for the 5 and 10 W/cm^2 irradiations such that αI corresponded to the linear values. For example, measurements of the linear absorption coefficient in mouse liver reported elsewhere in the literature (Drewniak et al. 1990; Parker 1988), yield a value of $\alpha = 0.033$ cm^{-1} ± 10%; hence, $\alpha I = 0.33$ W/cm^3, for $I = 10$ W/cm^2. Then, to obtain the same value of αI for a measured value of $\alpha = 0.059$ cm^{-1} in a nonlinear acoustic field, $I = 5.6$ W/cm^2. The additional heating resulting from nonlinear absorption at 0.5, 1.0 and 2.5 W/cm^2 is negligible, and these intensities are not scaled.

The temperature elevation in the fetus due to ultrasound exposure was determined by first establishing a thermal emf reference signal over 10 s during which no RF voltage was applied to the transducer, as shown in Figs. 2a and 2b. The sound was turned on by applying a predetermined voltage to the transducer

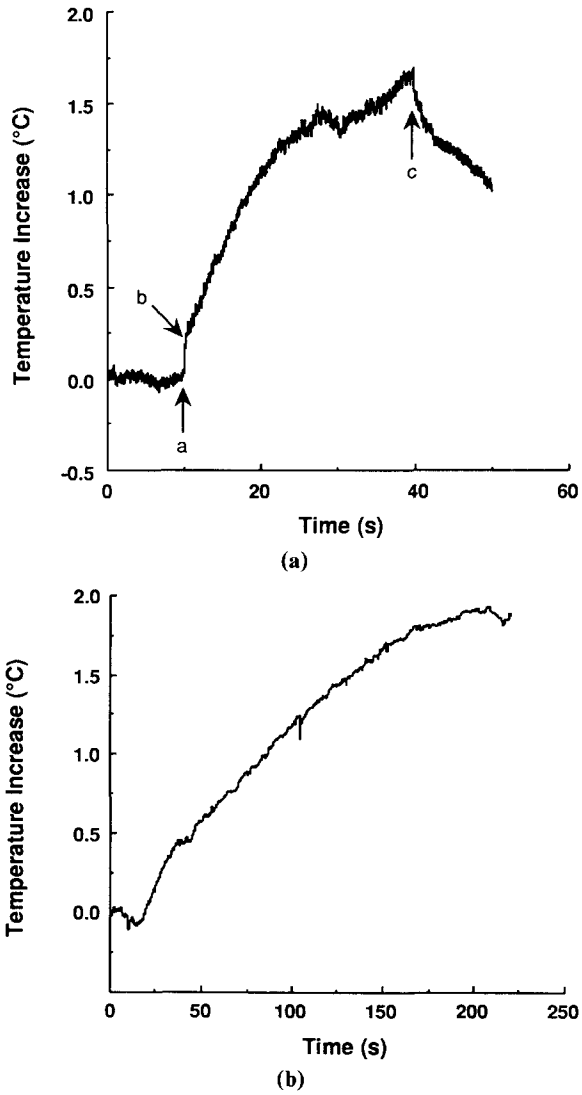

Fig. 2. Representative traces of temperature elevation data for (a) 15-day fetus exposed to 30 s at 10 W/cm^2, and (b) 12-day fetuses exposed for 200 s at 1 W/cm^2.

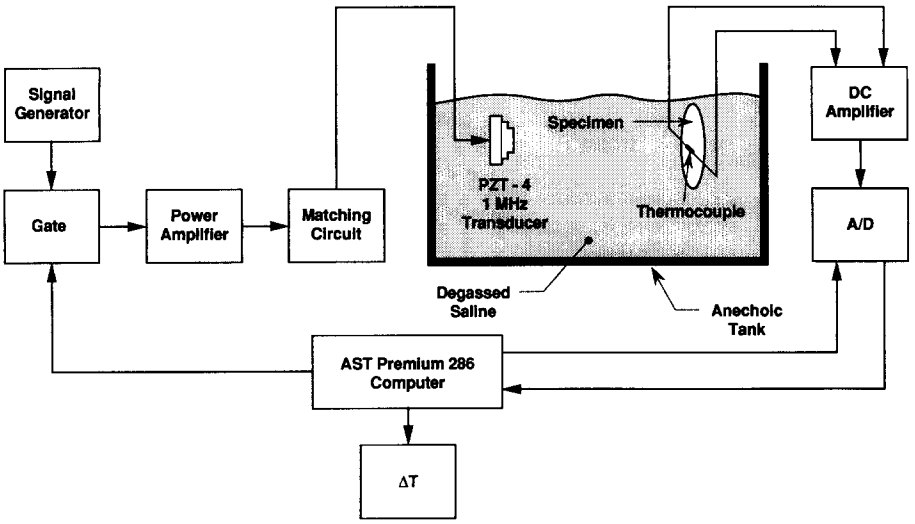

Fig. 3. Schematic representation of the measurement system.

after the reference period, for the prescribed exposure time. A 10-s decay period was sampled after the sound exposure was terminated. The thermal emf was amplified by a DC amplifier and digitized by a Metrabyte DAS-20 A/D converter. The voltage samples were averaged over the initial period with no ultrasound exposure to establish the reference temperature (assumed to be 37°C, the temperature of the dam and bath), and then averaged at the end of the exposure for 0.5 s for the 10 W/cm^2 intensity and 1 s for all other exposures. The temperature elevation was estimated by subtracting the reference voltage from the peak voltage and multiplying the result by the Seebeck coefficient for the thermocouple materials (Powell et al. 1975). The exposure system and data acquisition were controlled by an AST Premium 286 personal computer. A schematic of the measurement system is shown in Fig. 3.

Figures 2a and 2b are representative data traces of the temperature elevation, measured with the implanted thermocouples, upon exposure of the dam to ultrasound. In the cases shown, the exposures were at an SPTA acoustic intensity of 10 W/cm^2 for 30 s and 1 W/cm^2 for 200 s for Figs. 2a and 2b, respectively. The lower arrow *a* in Fig. 2a indicates the point at which the exposure was initiated after a 10-s reference signal. Viscous heating arising from the relative motion of the thermocouple wire and the tissue was seen to occur initially, as indicated by arrow *b*, followed by heating due to the absorption of ultrasound in the body of the tissue. The additional temperature increase resulting from the presence of the temperature sensor, which reaches its steady-state value very rapidly, was subtracted from the total temperature increase when it significantly biased the estimate of the temperature elevation due to ultrasonic absorption, as shown in Fig. 2a. The upper arrow *c* indicates the instant the ultrasound exposure was terminated. Fluctuations in the thermal emf output of the junction sometimes occur during the measurement period that are due to respiration or other movements by the dam. Such movements may change the location of the thermocouple junction relative to the ultrasound beam. Figure 2a shows an example of such fluctuations which do not affect significantly the determination of the temperature elevation.

Following the measurements, the animal and holder were removed from the tank. With the dam still under anesthesia, the abdomen was then opened surgically, and the location of the thermocouple junction in each fetus was determined with the aid of a dissecting microscope. The dam was then sacrificed by cervical dislocation.

MEASURED TEMPERATURE ELEVATIONS

The measured values of fetal temperature increase for each of the five ultrasound doses employed are shown in Table 1. The dose is defined as the product of the SPTA intensity and exposure duration $I_e t$. The intensity given in Table 1 is denoted as the SPTA effective intensity I_e to indicate that the effects of heating due to nonlinear absorption have been taken into account by scaling the intensity. Each datum point is the average of measurements made in at least 10 different specimens. Values obtained from measurements in the disk (area of placental attachment) and placement of the junction in the gestational sac, but not in the fetus, were also included. These areas are integral components of the feto-placental unit and will have a bearing on the well-being of the fetus. In addition, it is assumed, based on the measured data, that the temperature elevation at these points will not

Table 1. Measured versus computed temperature increase (°C) ± SD.

$I_e t$ (J/cm²)	I_e (W/cm²)	Exposure duration (s)	Perfusion constant τ for computed values (1/s)	Day of gestation 9 Measured	9 Computed	12 Measured	12 Computed	15 Measured	15 Computed
200	0.5	400	2000	2.0 ± 0.7	1.4	2.1 ± 0.6	1.3	1.5 ± 0.5	1.3
200	1	200	2000	1.9 ± 0.4	1.9	2.4 ± 0.7	1.9	2.2 ± 0.8	1.8
300	2.5	120	500	2.9 ± 1.2	3.2	3.1 ± 0.8	3.0	2.0 ± 0.9	3.0
300	10	30	100	3.4 ± 1.3	3.6	3.2 ± 1.0	3.4	2.1 ± 0.7	3.5
450	5	90	100	4.0 ± 1.2	3.8	3.9 ± 0.8	3.6	2.8 ± 0.6	3.6

I_e is the effective acoustic intensity to account for nonlinear absorption at I_e = 5 and 10 W/cm².

differ measurably from points in the fetus. Computed values of the temperature elevation discussed later are also given.

The temperature elevation in some cases was of the same magnitude, or greater than those previously shown to cause teratological effects in mice (Edwards 1986). Table 1 also shows that the temperature elevation is nearly equal in the 9- and 12-day fetuses, but less in most instances in the 15-day fetuses, as compared to the 9- and 12-day cases. This suggests that the earlier gestation fetuses are prone to temperature increases of greater magnitude from ultrasound exposure. The lower temperature increase in the 15-day fetuses is not presently understood. It is believed that absorption increases with fetal development because of the decreasing water content and increasing collagen and globular protein content as tissues develop, as well as bone development (Drewniak et al. 1989; Goss and Dunn 1980; Goss et al. 1980), which would lead one to expect greater heating. It is possible that the smaller size of the early gestation fetuses, relative to the beam dimension, and the increased fetal and maternal vascularizations in later gestation fetuses play a significant role that is not presently completely understood.

ANALYTICAL DEVELOPMENT

The bioheat equation, introduced by Pennes (1948), has been employed for calculating the temperature increase in soft tissue resulting from exposure to ultrasonic irradiation (Filipczynski 1977; Konopatskaya 1988; Lizzi and Ostromogilsky 1987; Nyborg 1988; Nyborg and Steele 1983), namely,

$$\frac{\partial T(\bar{\mathbf{r}}, t)}{\partial t} = \kappa \nabla^2 T(\bar{\mathbf{r}}, t) - \frac{T(\bar{\mathbf{r}}, t)}{\tau} + \frac{q_0 f(\bar{\mathbf{r}}) F(t)}{\rho C_p} \quad (1)$$

where $T(\bar{\mathbf{r}}, t)$ is the temperature increase at the point $\bar{\mathbf{r}} = (x, y, z)$ and time t, ρC_p is the volume-specific heat of the tissue, κ is the thermal diffusivity, τ is the blood perfusion time constant (inversely proportional to the blood perfusion rate w), q_0 is the rate of heat generation per unit volume, and $f(\bar{\mathbf{r}})$ and $F(t)$ are the spatial and temporal variations, respectively, of the heat source distribution.

A solution to eqn (1) for an infinite, homogeneous and isotropic medium can be found using transform techniques as (Davies 1978)

$$T(\bar{\mathbf{r}}, t) = \frac{q_0}{\rho C_p} \int_0^t d\xi F(\xi) \int_V d\bar{\mathbf{r}}' f(\bar{\mathbf{r}}') G(\bar{\mathbf{r}} - \bar{\mathbf{r}}', t - \xi) \quad (2)$$

where

$$G(\bar{\mathbf{r}} - \bar{\mathbf{r}}', t - \xi) = \frac{e^{-(t-\xi)/\tau - |\bar{r}-\bar{r}'|^2/4\kappa(t-\xi)}}{[4\pi\kappa(t-\xi)]^{3/2}} \quad (3)$$

is the appropriate Green's function (Stakgold 1979), $\bar{\mathbf{r}}'$ is the source variable coordinate and ξ is the temporal variable of the heat source function. The infinite, isotropic homogeneous Green's function given in eqn (3) is typically integrated over a sphere or cylinder with uniform heat generation to approximate the temperature elevation resulting from ultrasound exposure. This Green's function is employed in the analysis given later. Although the infinite, homogeneous and isotropic model is simple, it does allow for different heat source functions to be specified in the heating volume V (*e.g.*, specification of the absorption coefficient of the fetus as different from that of the dam). This solution does, however, assume that the blood perfusion is everywhere uniform. Although blood perfusion is known not to be uniform (Theiler 1983), it is a formidable task to find the appropriate Green's function for eqn (1) for an inhomogeneous region. Nonuniform blood perfusion could be included in the calculations if a numerical method (*e.g.*, a finite element analysis; see Axelsson and Barker 1984; Jaluria and Torrance 1986) were employed to determine the temperature elevation; however, current estimations of the temperature increase in fetal exposures to ultra-

sound are based on the solution given by eqn (2) (Nyborg 1988), and this approach is taken herein.

An attenuated traveling plane wave is typically assumed for acoustic propagation in soft tissue when computing the temperature increase. The equivalent heat source approximating the energy deposition resulting from ultrasonic absorption is then assumed to be

$$q_0 f(\bar{\mathbf{r}}) F(t) = 2\alpha I_0 e^{-\alpha z} f(x, y) U(t) \qquad (4)$$

where α is the ultrasonic absorption coefficient in soft tissue, I_0 is the SPTA intensity, $f(x, y)$ is the beam profile in the plane transverse to the direction of propagation (z direction) and $U(t)$ is the unit step function indicating a *CW* exposure. An unfocused piston ultrasound source was employed in this study. Previous studies have shown that the temperature increase on the axis of propagation, resulting from a piston source with a $[2J_1(ar)/ar]^2$ transverse beam profile (where $r^2 = x^2 + y^2$, and a is a beam width parameter), is not significantly different than a source with a Gaussian distribution (Carstensen et al. 1990; Drewniak et al. 1990). Because a Gaussian function can be treated analytically in performing the spatial integrals in eqn (2), the ultrasound intensity is assumed to vary as (Drewniak et al. 1990; Parker 1983; Parker and Lyons 1988)

$$I(\bar{\mathbf{r}}) = I_0 \exp(-\alpha z) \exp\left(-\frac{x^2 + y^2}{\beta_r}\right) \qquad (5)$$

where $\beta_r = (0.5\ HPBW)^2/ln2$ is the beam shape parameter in the radial dimension (*HPBW* denotes the 3-dB or half-power beam width). A Gaussian shape can also be included in the axial direction to approximate a focused beam. Analytical expressions for the acoustic field of transducers that radiate Gaussian beams have been given in the literature (Du and Breazeale 1985, 1987), and recent work has been published presenting analytical and numerical results of the temperature increase in tissue upon exposure to radiation from such sources (Wu and Du 1990). The analytical expressions for these beams are significantly more complicated to apply when calculating the heating due to ultrasound exposure than is eqn (5), and not readily amenable to planar source region boundaries.

In using the intensity distribution described by eqn (5), it is assumed that the shape of the ultrasound beam is not changed as it propagates through the tissue. Measurements in a homogeneous tissue such as liver suggest this is not the case exactly (Parker 1983). If a piecewise constant function of z is used for β_r, analytical simplifications for eqn (2) still result and allow for some changing of the profile. However, this may imply a better fit between the model and the experimental situation than is actually the case.

The spatial integrals in eqn (2) can be treated analytically for a separable Gaussian shape intensity profile if the source region is bounded by planar surfaces. Hence, the fetus and dam are modeled with rectangular absorbing volumes, as shown in Fig. 4. Let the source region V be defined by the three regions R_1, R_2 and R_3 with heat source functions q_1, q_2 and q_3 as

$$R_1 = \begin{cases} x_{1d} < x < x_{2d} \\ y_{1d} < y < y_{2d} \\ z_{1d} < z < z_{2d} \end{cases}$$

$$q_1(x, y, z) = 2\alpha_d I_0 \exp(-2\alpha_d (z - z_{1d})) \times \exp\left(-\frac{x^2 + y^2}{\beta_r}\right)$$

$$R_2 = \begin{cases} x_{1f} < x < x_{2f} \\ y_{1f} < y < y_{2f} \\ z_{1f} < z < z_{2f} \end{cases}$$

$$q_2(x, y, z) = 2\alpha_d I_0 \exp[-2\alpha_d (z_{1f} - z_{1d}) - 2\alpha_f (z - z_{1f})] \exp\left(-\frac{x^2 + y^2}{\beta_r}\right)$$

$$R_3 = \begin{cases} x_{1f} < x < x_{2f} \\ y_{1f} < y < y_{2f} \\ z_{2f} < z < z_{2d} \end{cases}$$

$$q_3(x, y, z) = 2\alpha_d I_0 \exp[-2\alpha_d (z_{1f} - z_{1d}) - 2\alpha_f (z_{2f} - z_{1f}) - 2\alpha_d (z - z_{2f})] \exp\left(-\frac{x^2 + y^2}{\beta_r}\right)$$

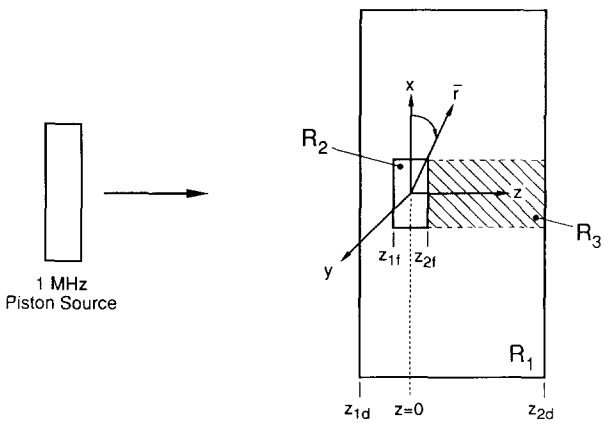

Fig. 4. Coordinates and heat source volumes used in the analytical treatment of the temperature elevation.

where R_1 is the entire volume of the larger rectangular parallelpiped, R_2 is the volume of the smaller rectangular parallelpiped modeling the fetus and R_3 is the "shadow" region behind the smaller rectangular parallelpiped. The coordinates x_{1d}, x_{2d}, y_{1d} etc. are the planes bounding the parallelpipeds employed to approximate the dam and fetus, and the indices d and f denote the boundaries approximating the dam and fetus, respectively. The temperature increase for this heat source is then given by

$$T(\bar{\mathbf{r}}, t) = \frac{t}{\rho C_p}\int_0^1 d\xi\Big\{\int_{R_1} d\bar{\mathbf{r}}' q_1(\bar{\mathbf{r}}')G(\bar{\mathbf{r}}-\bar{\mathbf{r}}', t\xi) - \int_{R_2+R_3} d\bar{\mathbf{r}}' q_1(\bar{\mathbf{r}}')G(\bar{\mathbf{r}}-\bar{\mathbf{r}}', t\xi) + \int_{R_2} d\bar{\mathbf{r}}' q_2(\bar{\mathbf{r}}')G(\bar{\mathbf{r}}-\bar{\mathbf{r}}', t\xi) + \int_{R_3} d\bar{\mathbf{r}}' q_3(\bar{\mathbf{r}}')G(\bar{\mathbf{r}}-\bar{\mathbf{r}}', t\xi)\Big\} \quad (6)$$

where a unit step ultrasonic exposure has been assumed, and a change of variables $t\xi = t - \theta$ has been introduced in eqn (2). Upon performing the spatial integrals, the temperature increase is given by

$$\begin{aligned}
T(\bar{\mathbf{r}}, t) &= \frac{2\alpha_d I_0}{\rho C_p} te^{2\alpha_d z_{1d}} \\
&\times \int_0^1 d\xi\{e^{-t\xi/\tau}L(\bar{\mathbf{r}}, t\xi, \alpha_d) \\
&\times [M(t\xi, x, x_{1d}) - M(t\xi, x, x_{2d})] \\
&\times [M(t\xi, y, y_{1d}) - M(t\xi, y, y_{2d})] \\
&\times [N(t\xi, \alpha_d, z, z_{1d}) - N(t\xi, \alpha_d, z, z_{2d})]\} \\
&+ \frac{2\alpha_f I_0}{\rho C_p} te^{-2\alpha_d(z_{1f}-z_{1d})+2\alpha_f z_{1f}} \\
&\times \int_0^1 d\xi\{e^{-t\xi/\tau}L(\bar{\mathbf{r}}, t\xi, \alpha_f) \\
&\times [M(t\xi, x, x_{1f}) - M(t\xi, x, x_{2f})] \\
&\times [M(t\xi, y, y_{1f}) - M(t\xi, y, y_{2f})] \\
&\times [N(t\xi, \alpha_f, z, z_{1f}) - N(t\xi, \alpha_f, z, z_{2f})]\} \\
&+ \frac{2\alpha_d I_0}{\rho C_p} te^{-2\alpha_d(z_{1f}-z_{1d})-2\alpha_f(z_{2f}-z_{1f})+2\alpha_d z_{2f}} \\
&\times \int_0^1 d\xi\{e^{-t\xi/\tau}L(\bar{\mathbf{r}}, t\xi, \alpha_d) \\
&\times [M(t\xi, x, x_{1f}) - M(t\xi, x, x_{2f})] \\
&\times [M(t\xi, y, y_{1f}) - M(t\xi, y, y_{2f})] \\
&\times [N(t\xi, \alpha_d, z, z_{2f}) - N(t\xi, \alpha_d, z, z_{2d})]\} \\
&- \frac{2\alpha_d I_0}{\rho C_p} te^{-2\alpha_d z_{1d}} \\
&\times \int_0^1 d\xi\{e^{-t\xi/\tau}L(\bar{\mathbf{r}}, t\xi, \alpha_d) \\
&\times [M(t\xi, x, x_{1f}) - M(t\xi, x, x_{2f})] \\
&\times [M(t\xi, y, y_{1f}) - M(t\xi, y, y_{2f})] \\
&\times [N(t\xi, \alpha_d, z, z_{1f}) - N(t\xi, \alpha_d, z, z_{2d})]\} \quad (7)
\end{aligned}$$

where

$$L(\bar{\mathbf{r}}, t\xi, \alpha_i) = \frac{e^{-((x^2+y^2/\beta_r)(1/1+(4\kappa t\xi/\beta_r)))}}{1+\frac{4\kappa t\xi}{\beta_r}} e^{-(2\alpha_i z - 4\alpha_i^2 \kappa t\xi)}$$

$$M(t\xi, v, v_{mn}) = \frac{1}{2} erf\left[\frac{1}{\sqrt{4\kappa t\xi}}\left(1+\frac{4\kappa t\xi}{\beta_r}\right)^{1/2}\left(\frac{1}{1+\frac{4\kappa t\xi}{\beta_r}}v - v_{mn}\right)\right]$$

$$N(t\xi, \alpha_i, z, z_{mn}) = \frac{1}{2} erf\left[\frac{1}{\sqrt{4\kappa t\xi}}(z - 4\alpha_i \kappa t\xi - z_{mn})\right].$$

The differences between this particular method of modeling the ultrasound beam and absorbing region over solutions given by other investigators include the shape of the beam, incorporation of plane wave attenuation in the intensity function and allowance for a different absorption coefficient in the fetus compared to that for the surrounding tissues of the dam (Abraham et al. 1989; Nyborg and Steele 1983). The source region has been approximated with rectangular parallelpipeds as opposed to spherical or cylindrical regions to enable analytical integration of the volume integrals for the described heat source (Abraham et al. 1989; Nyborg and Steele 1983).

DISCUSSION

The mouse is a suitable animal model for this study despite maternal size differences because the mouse and the human have the same type of placentation, namely, hemochorial (Kirby and Bradbury 1965; Rugh 1968). Also, while body size differences between the mouse and human fetus are great in the later gestation fetuses, they are comparable in the very early gestation embryo. Recent reports tell that transvaginal ultrasound is being used to detect human em-

bryos with a crown–rump length as small as 2 mm (Dakin 1990) corresponding to a gestational age of 3 weeks (Arey 1974). The crown–rump length of the 9-day mouse embryos measured in this study was 3 mm and comparable in development to a 25- to 26-day human embryo (Rugh 1968).

Although vascularization increases during placental development, the uterine blood flow rate reaches a maximum on day 3 of pregnancy in the mouse (Bindon 1969) and on day 14–15 in the human (Wilkin 1965). Approximately 20% of the incoming uterine blood flows to the myometrium and endometrium and the other 80% to the area of placental attachment (Resnik 1989). The blood flow volume increases due to the increase in the size of the placenta and uterus during gestation, particularly in the latter half of gestation. The blood flow per unit weight, however, remains constant (Resnik 1989).

The fetus is dependent on conduction to adjoining maternal tissues to remove heat, which is then carried off by maternal blood flow (Fisher 1989; McGrail and Seagrave 1980). The mechanics of circulation in this case are not conducive to rapid perfusion and thus heat removal. Briefly, placental blood enters from the uterine arteries under high pressure in jetlike spurts and flows into the intervillous spaces. Blood flow in the intervillous space is slowed significantly, forming pools to allow time for exchange of nutrients and waste products from the chorionic villi. This blood is then forced into the uterine venous system by new incoming arterial blood (Bloom and Fawcett 1975; Wilkin 1965). The continually increasing fetal temperature during the ultrasound exposures used in this study is an indication that heat is not rapidly removed as would be the case for well-perfused tissues such as the adult ovary (Bailey et al. 1987).

Although the data indicate that the temperature increase is related approximately linearly to the dose, It, this is not expected. If the source terms q_1, q_2 and q_3 are substituted into eqn (6), it is observed that

$$T(\bar{\mathbf{r}}, t) \propto Itv(\bar{\mathbf{r}}, t, \alpha_i, \tau, R_i) \qquad (8)$$

where the R_i are the source regions. Then v is a function of time as well as other quantities. The perfusion constant τ is expected to be a function of temperature, and hence will also be time dependent. Thus, the linear relation observed between the energy flux It and the temperature elevation is not expected from the analysis.

The computed temperature increases are also shown in Table 1 (in parentheses) and can be compared to the measured values. The size of the rectangular parallelpiped employed to approximate the dam is $5 \times 4 \times 2$ cm ($x_{1d} = -2.5$, $x_{2d} = 2.5$; $y_{1d} = -2$, $y_{2d} = 2$; $z_{1d} = -0.35$, $z_{2d} = 1.65$), and the absorption coefficient is taken to be 0.035 cm^{-1}, a reported value for the absorption coefficient in liver (Drewniak 1991; Lyons and Parker 1988). The sizes of the rectangular parallelpipeds approximating the fetuses are $5 \times 3 \times 3$ mm ($x_{1f} = -0.25$, $x_{2f} = 0.25$; $y_{1f} = -0.15$, $y_{2f} = 0.15$; $z_{1f} = -0.15$, $z_{2f} = 0.15$), $8 \times 5 \times 5$ mm and $15 \times 9 \times 9$ mm for the 9-, 12- and 15-day fetuses, respectively. The coordinates are chosen to allow for a 2-mm thickness of the uterine wall in the propagation path between the water interface and the fetus, although for an absorption coefficient of 0.035 cm^{-1} the resulting attenuation is small. The absorption coefficient for the three gestational ages are taken, respectively, to be 0.018, 0.023 and 0.028 cm^{-1}. This corresponds to a linear function of gestational age, where on day 19 (birth) the absorption coefficient for this function would be 0.035 cm^{-1}. The perfusion constant τ was chosen to be different for the various exposure times and intensities to obtain agreement between the measured and computed temperature increases. Immediate increases in the blood flow following the initiation of the exposure might be expected at the higher intensities and shorter exposure times as a result of the rapid temperature increase. Hence, a high perfusion rate (τ = 100 s) is chosen (Sekins and Emery 1982). At the longer exposure times and lesser intensities where the rate of temperature increase is slower, a lesser perfusion rate (τ = 2000 s) is used. A moderate rate of perfusion (τ = 500 s) is chosen for the intermediate exposure time and intensity. In all cases, the rate

Table 2. Computed temperature increase for different perfusion constants (°C).

I_{SPTA} (W/cm^2)	Exposure duration (s)	τ (1/s)					
		100	200	500	1000	2000	∞
0.5	400	0.5	0.8	1.1	1.2	1.3	1.4
1	200	0.9	1.3	1.6	1.7	1.8	1.9
2.5	120	2.0	2.6	3.0	3.1	3.2	3.3
10	30	3.5	3.8	3.9	4.0	4.0	4.0
5	90	3.6	4.3	4.9	5.1	5.2	5.3

of perfusion could be expected to be a function of the temperature and the rate of temperature increase, and hence time. Such details, however, are presently not available. The effect of perfusion on the temperature elevation is shown in Table 2 for the parameters of the 15-day fetuses used in the computations. At short exposure times, even a high perfusion rate (τ = 100 s) affects the total temperature elevation only slightly, whereas for longer exposure times the rate of perfusion affects the temperature increase significantly, as would be expected.

The computed elevation is nearly equal to or greater than the measured increases at the higher doses. However, at the lower doses, which are more likely to occur clinically, and for the younger gestational ages, which are more susceptible to thermal insult, the computed temperature elevation is lower than or comparable to the measured values. The comparison between the measured temperature elevation and model calculations, while being reasonable, emphasizes that exposure criteria based on such calculations should be conservative. It is clear that the model from which the computed results are obtained is overly simple relative to the actual experimental physiological situation. A more realistic model would include better determination and modeling of the ultrasound beam as it propagates and impinges on the fetus. Nonuniform blood flow and reasonable approximations of absorption coefficients and perfusion rates also need to be included. Although the absorption coefficient, which affects the calculations primarily as a scale factor outside the integral in eqn (7), and the perfusion time constant τ, can be chosen to fit approximately most experimental data obtained in a manner such as that of this study. An attempt was made, however, to present reasonable arguments for the values of absorption coefficients and perfusion constants assumed for the model calculations.

Significant risk of heating could occur in the early gestation exposures, as the embryo is very small relative to the beam size, even for the focused beams used clinically, and the ability to remove heat is more poorly developed than in later gestation fetuses. Ultrasound exposure conditions, which may result in insignificant heating of a later gestation fetus, could be quite harmful to the early embryo. As development of technology provides for imaging earlier in gestation, clinicians need to be provided with accurate information detailing the risk of heating the embryo at this vulnerable gestational age.

REFERENCES

Abraham, V.; Ziskin, M. C.; Heynen, S. Temperature elevation in the rat fetus due to ultrasound exposure. Ultrasound Med. Biol. 15:443–449; 1989.

Arey, L. B. Development anatomy. Philadelphia: W. B. Saunders Co.; 1974.

Axelsson, O.; Barker, V. A. Finite element solution of boundary value problems. New York: Academic Press, Inc.; 1984.

Bacon, D. R.; Carstensen, E. L. Increased heating by diagnostic ultrasound due to nonlinear propagation. J. Acoust. Soc. Am. 88:26–34; 1990.

Bailey, K. I.; O'Brien, W. D., Jr.; Dunn, F. Ultrasonically induced temperature elevation in mouse ovary. Ultrasound Med. Biol. 10:492–499; 1984. (Reprinted correctly, Ultrasound Med. Biol. 13:29–31; 1987.)

Bindon, B. M. Blood flow in the reproductive organs of the mouse after hypophysectomy, after gonadotrophin treatment, during the estrous cycle, and during early pregnancy. J. Endocr. 44:523–536; 1969.

Blackstock, D. T. Connection between the Fay and Fubini solutions for plane sound waves of finite amplitude. J. Acoust. Soc. Am. 39:1019–1026; 1966.

Bloom, W.; Fawcett, D. W. A. Textbook of histology. Philadelphia: W. B. Saunders Co.; 1975.

Brix, K. A. Environmental and occupational hazards to the fetus. J. Reprod. Med. 27:577–583; 1982.

Carstensen, E. L.; Child, S. Z.; Norton, S.; Nyborg, W. Ultrasonic heating of the skull. J. Acoust. Soc. Am. 87:1310–1317; 1990.

Carstensen, E. L.; Dalecki, D.; Parker, K. J.; Bacon, D. R.; Blackstock, D. Nonlinear aspects of ultrasonic heating. J. Acoust. Soc. Am. 86(Suppl. 1):S27; 1989.

Carstensen, E. L.; Law, W. K.; McKay, N. D.; Muir, T. G. Demonstration of nonlinear acoustical effects at biomedical frequencies and intensities. Ultrasound Med. Biol. 6:359–368; 1980.

Carstensen, E. L.; McKay, N. D.; Dalecki, D.; Miur, T. G. Absorption of finite amplitude ultrasound in tissues. Acustica. 51:116–123; 1982.

Dakin, D. R. Endovaginal ultrasound abets fetal assessment. Diag. Imaging. 12:71–79; 1990.

Dalecki, D.; Carstensen, E. L.; Parker, K. J.; Bacon, D. R. Overview of absorption of finite amplitude, focused ultrasound. In: Hamilton, M. F.; Blackstock, D. T., eds. Frontiers of nonlinear acoustics: Proceedings of the 12th ISNA. London: Elsevier Science Publishers Ltd.; 1990:125–130.

Davies, B. Integral transforms and their applications. New York: Springer-Verlag; 1978:47–50.

Drewniak, J. L. Ultrasonic absorption of soft and hard fetal tissues. University of Illinois; 1991. Thesis.

Drewniak, J. L.; Carnes, K. I.; Dunn, F. *In vitro* ultrasonic heating of fetal bone. J. Acoust. Soc. Am. 86:1254–1258; 1989.

Drewniak, J. L.; Frizzell, L. A.; Dunn, F. Errors resulting from finite beamwidth and sample dimensions in the determination of the ultrasonic absorption coefficient. J. Acoust. Soc. Am. 88:967–977; 1990.

Du, G.; Breazeale, M. A. The ultrasonic field of a Gaussian transducer. J. Acoust. Soc. Am. 78:2083–2086; 1985.

Du, G.; Breazeale, M. A. Theoretical description of a focussed Gaussian ultrasonic beam in a nonlinear medium. J. Acoust. Soc. Am. 81:51–57; 1987.

Dunn, F.; Averbuch, A. J.; O'Brien, W. D., Jr. A primary method for the determination of ultrasonic intensity with the elastic sphere radiometer. Acustica. 38:58–61; 1977.

Edmonds, P. D.; Stolzenberg, S. J.; Torbin, C. A.; Maden, S. M.; Pratt, D. E. Postpartum survival of mice exposed *in utero* to ultrasound. J. Acoust. Soc. Am. 66:590–593; 1979.

Edwards, M. J. Hyperthermia as a teratogen: A review of experimental studies and their clinical significance. Terat. Carcinog. Mutag. 6:568–582; 1986.

Filipczynski, L. Thermal effects in soft tissues developed under the action of ultrasonic fields of long durations. Archives Acoust. 2:297–303; 1977.

Fisher, B. R. Biological effects of hyperthermia and potential risk associated with ultrasound exposure. FDA CDRH Publ. PB90 10 070; 1989.

Fry, F. J.; Dines, K. A.; Rielly, C. R.; Goss, S. A. Losses in tissue

associated with finite amplitude ultrasound transmission. Ultrasound Med. Biol. 15:481–497; 1989.

Fry, W. J.; Dunn, F. Ultrasound: Analysis and experimental methods in biological research. In: Nastuck, W. L., ed. Physical techniques in biological research. Vol. 4. New York: Academic Press, Inc.; 1962:261–394.

Fry, W. J.; Fry, R. B. Determination of absolute sound levels and acoustic absorption coefficients by thermocouple probes—experiment. J. Acoust. Soc. Am. 26:311–317; 1954a.

Fry, W. J.; Fry, R. B. Determination of absolute sound levels and acoustic absorption coefficients by thermocouple probes—theory. J. Acoust. Soc. Am. 26:294–310; 1954b.

Goss, S. A.; Dunn, F. Ultrasonic propagation properties of collagen. Phys. Med. Biol. 25:827–837; 1980.

Goss, S. A.; Frizzell, L. A.; Dunn, F.; Dines, K. A. Dependence of the ultrasonic properties of biological tissue on constituent proteins. J. Acoust. Soc. Am. 67:1041–1044; 1980.

Goss, S. A.; Fry, F. J. Nonlinear acoustic behavior in focused ultrasonic fields: Observations of intensity dependent absorption in biological tissue. IEEE Trans. Sonics Ultrason. 28:21–26; 1981.

Hamilton, M. F. Fundamentals and applications of nonlinear acoustics. In: Wright, T. W., ed. Nonlinear wave propagation in mechanics. New York: The American Society of Mechanical Engineers; 1986:1–28.

Jaluria, Y.; Torrance, K. E. Computational heat transfer. Washington, DC: Hemisphere Publishing; 1986.

Kirby, D. R. S.; Bradbury, S. The hemo-chorial mouse placenta. Anat. Rec. 152:279–282; 1965.

Konopatskaya, I. I. Theoretical investigation of the local heating of biological tissue under the action of focused ultrasound. Sov. Phys. Acoust. 34:384–387; 1988.

Lele, P. P. Ultrasonic teratology in mouse and man. Proceedings of the Second European Congress on Ultrasonics in Medicine, Munich, Germany, International Congress Series No. 363. Amsterdam: Excerpta Medica; 1975:22–27.

Lele, P. P. Safety and potential hazards in the current applications of ultrasound in obstetrics and gynecology. Ultrasound Med. Biol. 5:307–320; 1979.

Lizzi, F. L.; Ostromogilsky, M. Analytical modeling of ultrasonically induced tissue heating. Ultrasound Med. Biol. 13:607–618; 1987.

Lyons, M. E.; Parker, K. J. Absorption and attenuation in soft tissues: II—experimental results. IEEE Trans. Ultrason. Ferroelectr. Freq. Contr. UFFC-35:511–521; 1988.

McGrail, T. W.; Seagrave, R. C. Application of the bioheat transfer equation in fetal placental studies. Ann. NY Acad. Sci. 335:161–172; 1980.

Miller, M. W.; Ziskin, M. C. Biological consequences of hyperthermia. Ultrasound Med. Biol. 15:707–722; 1989.

Muir, T. G.; Carstensen, E. L. Prediction of nonlinear acoustic effects at biomedical frequencies and intensities. Ultrasound Med. Biol. 6:345–347; 1980.

Nyborg, W. L. Solutions of the bio-heat transfer equation. Phys. Med. Biol. 33:785–792; 1988.

Nyborg, W. L.; Steele, R. B. Temperature elevation in a beam of ultrasound. Ultrasound Med. Biol. 9:611–620; 1983.

Parker, K. J. The thermal pulse decay technique for measuring ultrasonic absorption coefficients. J. Acoust. Soc. Am. 74:1356–1361; 1983.

Parker, K. J. Ultrasonic attenuation and absorption in liver tissue. Ultrasound Med. Biol. 9:363–369; 1983.

Parker, K. J.; Lyons, M. E. Absorption and attenuation in soft tissues: I—calibration and error analyses. IEEE Trans. Ultrason. Ferroelectr. Freq. Contr. UFFC-35:242–252; 1988.

Pennes, H. H. Analysis of tissue and arterial blood temperatures in resting human forearm. J. Appl. Physiol. 2:93–122; 1948.

Powell, R. L.; Hall, W. J.; Hyink, C. H.; Sparks, L. L.; Burns, G. W.; Scroger, M. G.; Plumb, H. H. Thermocouple reference tables based on the IPTS-68, National Bureau of Standards monograph no. 125. Stamford: Omega Press; 1975.

Resnik, R. Anatomic alterations in the reproductive tract. In: Creasy, R. K.; Resnik, R., eds. Maternal-fetal medicine: Principles and practice. Philadelphia: W. B. Saunders Co.; 1989:136–140.

Rugh, R. The mouse: Its reproduction and development. Minneapolis: Burgess Publishing Company; 1968.

Sekins, K. M.; Emery, A. F. Thermal science for physical medicine. In: Lehman, J. F., ed. Therapeutic heat and cold. Baltimore: Williams and Wilkins; 1982:70–132.

Sikov, M. R.; Collins, D. H.; Carr, D. B. Measurement of temperature rise in prenatal rats during exposure of the exteriorized uterus to ultrasound. IEEE Trans. Sonics Ultrason. SU-31:497–503; 1984.

Smith, D. W.; Clarren, S. K.; Harvey, M. A. S. Hyperthermia as a possible teratogenic agent. J. Ped. 92:878–883; 1978.

Stakgold, I. Green's functions and boundary value problems. New York: John Wiley and Sons; 1979:488–489.

Stolzenberg, S. J.; Torbit, C. A.; Edmonds, P. D.; Taenzer, J. C. Effects of ultrasound on the mouse exposed at different stages of gestation: Acute studies. Rad. and Envir. Biophys. 17:245–270; 1980.

Theiler, K. Embryology. In: Foster, H. L.; Small, T. D.; Fox, J., eds. The mouse in biomedical research, vol. III: Normative, biology, immunology, and husbandry. Orlando, FL: Academic Press, Inc.; 1983:121–136.

Whittingham, D. G.; Wood, M. J. Reproductive physiology. In: Foster, H. L.; Small, T. D.; Fox, J., eds. The mouse in biomedical research, vol. III: Normative, biology, immunology, and husbandry. Orlando, FL: Academic Press, Inc.; 1983:137–146.

Wilkin, P. G. Organogenesis of the human placenta. In: DeHaan, R. L.; Ursprung, H., eds. Organogenesis. Chicago: Holt, Rinehart and Winston, Inc.; 1965:743–769.

Wu, J.; Du, G. Temperature elevation generated by a focused Gaussian beam of ultrasound. Ultrasound Med. Biol. 16:489–498; 1990.